analytical chemistry

pubs.acs.org/ac Letter

Particle Size Regulation of Single-Crystalline Covalent Organic Frameworks for High Performance of Gas Chromatography

Zi-Han Wang, Cheng Yang, Tianxi Liu, Hai-Long Qian,* and Xiu-Ping Yan

Cite This: *Anal. Chem.* 2023, 95, 8145−8149 Read Online

ACCESS | Metrics & More | Article Recommendations | Supporting Information

ABSTRACT: Although polycrystalline covalent organic frameworks (PCOFs) have already shown great potential as stationary phases for chromatography, irregular shape and size distribution of PCOFs make regulation of particle size of PCOFs for high separation performance impossible, which is accessible by the application of single-crystalline COFs (SCOFs). Herein, we showed preparation of three-dimensional SCOF (SCOF-303) bonded capillaries (SCOF-303-capillary) with different particle sizes (about 0.4−1.6 μm) and further investigated gas chromatographic separation ability of these SCOF-303-capillaries for isomers of xylene, dichlorobenzene, and pinene. It was found resolution and column efficiency of SCOF-303-capillaries for isomers decreased with the increase in particle size, mainly resulting from the weaker size-exclusion effect and higher mass transfer resistance of the larger particle size of flexible SCOF-303. The obtained SCOF-303-capillary (particle size of ∼0.4 μm) offered baseline separation of xylene isomers with the high resolution of 2.26−3.52, great efficiency of 7879 plates m^{-1} for *p*-xylene, better than PCOF-303-capillary, and commercial DB-5 and HP-FFAP capillary columns as well as many reported capillaries. This work not only shows the great potential of SCOFs for gas chromatography but also provides the theoretical direction for the design of the efficient COF based stationary phase by adjusting the particle sizes.

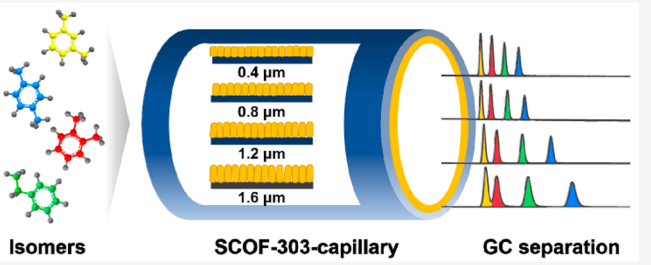

Improving separation ability by development of a novel stationary phase has always been the significant direction of chromatography.[1−4] The accessible designability of covalent organic frameworks (COFs) in topology, pore, and functionality at the molecular level makes COFs highly promising as stationary phases for chromatography.[5−7] In contrast to the traditional stationary phase, relying on the relatively single force of van der Waals force or polarity, COFs can introduce synergistic effects of multiple forces including molecular sieve, hydrophobic, hydrogen bonding, $\pi-\pi$ and C−H···π interactions, et al. to efficiently promote separation performance. Accordingly, diverse COFs were designed to serve as stationary phases and revealed a better resolution of isomers and enantiomers than traditional commercial stationary phases.[8−13] However, all the applied COFs for chromatography are polycrystalline. Crystal defect, irregular shape, and size distribution of polycrystalline COFs (PCOFs) not only limit interaction of analytes and COFs but also regulate particle size to make high chromatographic separation performance impossible.[14]

Single-crystalline COFs (SCOFs) refer to the whole crystal and are composed of the same spatial lattice in a three-dimensional direction, resulting in the long-range order of SCOF particles.[15−18] The complete and regular crystal structure makes pore blockage and mass transfer resistance of SCOFs less than PCOFs promoting the chromatographic separation performance of SCOFs.[16,19−21] For instance, SCOF-300 has already been employed as a stationary phase in liquid chromatography and gave excellent resolution for positional isomers.[22] Benzene and cyclohexane can be well separated on single-crystalline TAPPy-PDA and TABB-DMPDA COFs rather than the same polycrystalline materials.[14] More importantly, the regular particle size of SCOFs can be controlled by changing the growth time of the crystal, leading to accessible investigation of the effect of COF particle size on chromatographic separation performance, which has not been reported yet.

Herein, we intended to prepare SCOF bonded capillaries with different particle sizes and investigated gas chromatographic (GC) separation ability of these capillaries. A model single-crystalline three-dimensional COF (SCOF-303) was prepared by the condensation of tetrakis(4-formylphenyl)-methane (TFPM) and phenylenediamine (PDA) with aniline as the additive inhibitor. Aniline can compete with the precursor monomer of PDA to prevent a direct and rapid reaction between PDA and TFPM. Excess aniline would

Received: April 10, 2023
Accepted: May 12, 2023
Published: May 16, 2023

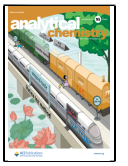

https://doi.org/10.1021/acs.analchem.3c01550
Anal. Chem. 2023, 95, 8145−8149

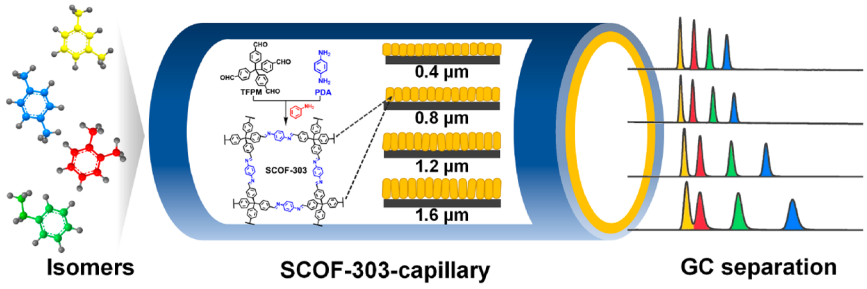

Figure 1. Design and preparation of SCOF-303-capillaries with different particle sizes to investigate the effect of particle size on the GC separation.

regulate the nucleation rate of COF-303, facilitating the formation of single crystals. Then, the SCOF-303 bonded capillary (SCOF-303-capillary) was prepared via an in situ growth approach. Particle size of SCOF-303 on the capillary was controlled by the growth time. Separation ability of the SCOF-303-capillaries with different particle sizes was assessed with positional isomers including xylene, dichlorobenzene (DCB), and pinene (Figure 1).

The experimental powder X-ray diffraction (PXRD) pattern of the synthesized SCOF-303 was consistent with that of the reported one.[10] Compared with polycrystalline COF-303 (PCOF-303) (Figure S1), SCOF-303 gave a narrower full width at half maxima (fwhm) of the characteristic PXRD peaks. The fwhm of PXRD peaks at 7.4° and 19.0° for SCOF-303 decreased from 0.44° to 0.36° and 0.40° to 0.35° with an increase in the reaction time from 15 to 30 days, respectively (Table S1). The results indicate a long reaction time is beneficial for the crystallinity of SCOF-303 (Figure 2a).

According to scanning electron microscope (SEM) images, the morphology of PCOF-303 was irregular (Figure S2), while SCOF-303 gave a uniform rectangular bar-like shape. With an increase in the reaction time from 15 to 30 days, particle size of SCOF-303 was enlarged from 1.0 to 5.5 μm (Figure S3), proving the available adjustment of particle size of SCOF-303 with the reaction time.

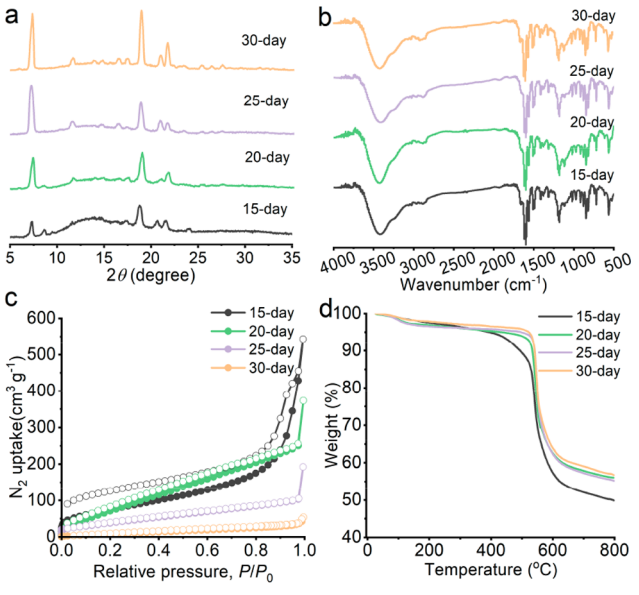

Figure 2. (a) PXRD patterns, (b) FT-IR spectra, (c) N_2 adsorption−desorption isotherms, and (d) thermogravimetric analysis of SCOF-303 synthesized with different reaction times.

The appearance of the characteristic imine band at 1625 cm^{-1} in the Fourier Transform-Infrared (FT-IR) spectra of SCOF-303 demonstrates successful Schiff-base condensation of TFPM and PDA. No obvious change in the shape of FT-IR between SCOF-303 formed with different reaction times indicates the same composition of these SCOF-303's (Figures 2b and S4).

Porosity and surface area of the prepared SCOF-303 were evaluated by nitrogen adsorption−desorption measurements. The BET surface area of PCOF-303 was revealed to be 490 m^2 g^{-1} (Figure S5). In contrast, SCOF-303 gave a lower BET surface area (340−42 m^2 g^{-1}) (Figure 2c). The larger crystal went against the dynamical structure change of COF-303 for adsorption of nitrogen, resulting in the decrease in the BET surface area.[16]

Thermogravimetric analysis showed SCOF-303 and PCOF-303 can maintain the weight within 540 and 450 °C, respectively (Figures 2d and S6). The high stability laid the foundation for application of COF-303 as a stationary phase for GC.

Owing to the regular particle size and high thermal stability of SCOF-303, a series of SCOF-303 bonded capillaries with different particle sizes were fabricated with the in situ growth approach to investigate the effect of particle size on the GC separation and obtain the SCOF based capillary with high separation performance. In order to avoid the blockage of the capillary, the concentration of monomers of SCOF-303 for preparation of the GC capillary was diluted four times.

SEM images of SCOF-303-capillaries revealed that uniform SCOF-303 was successfully grown onto the capillaries (Figure 3), while particles of PCOF-303-capillary exhibited an irregular shape (Figure S7). Like the single-crystalline powder, the crystal size of the capillary also can be controlled by the growth time. Several SCOF-300-capillaries with different particle sizes (0.4, 0.8, 1.2, and 1.6 μm) were obtained. The appearance of characteristic peaks of SCOF-303 in the PXRD pattern of SCOF-303-capillary demonstrates crystallinity of the particle growth (Figure S8). Furthermore, SCOF-303-capillary gave obvious FT-IR peaks of SCOF-303 and a bare silica capillary, indicating the successful synthesis of SCOF-303-capillary (Figure S9).

The prepared SCOF-303-capillaries were assessed with the probes of benzene (X), n-butanol (Y), 2-pentanone (Z), 1-nitropropane (U), and pyridine (S) to obtain the McReynolds constants (Table S2).[23] All of the SCOF-303-capillaries were proved to be nonpolar, and the polarity remained not significantly different owing to the same composition of the stationary phase. The small values of Y and Z indicate the weak

https://doi.org/10.1021/acs.analchem.3c01550
Anal. Chem. 2023, 95, 8145−8149

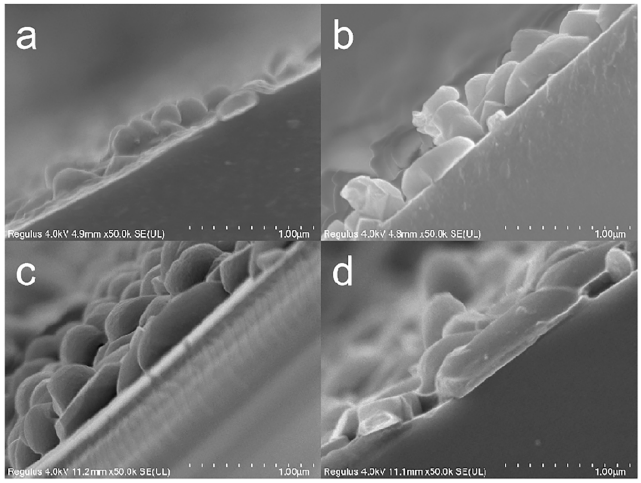

Figure 3. SEM images of SCOF-303-capillaries with different reaction times: (a) 15-day, (b) 20-day, (c) 25-day, and (d) 30-day.

interaction between SCOF-303 and the analyte with the proton-donor/acceptor, while the large value of X reflects the strong $\pi-\pi$ interaction force of SCOF-303.[23,24]

In order to explore the effect of particle size on separation performance of SCOF-capillaries, we further studied GC separation of isomers including xylene, DCB, and pinene on the prepared SCOF-303-capillaries. The separation performance of SCOF-303-capillaries varied with different particle sizes (Figures 4a-4b). As for xylene isomers, resolution (R) of *m*-xylene and *o*-xylene decreased from 2.55 to 1.23 with an increase in the particle size from 0.4 to 1.6 μm (Table S3). SCOF-303 at 1.6 μm gave no baseline separation of *m*-xylene and *o*-xylene. In addition, the theoretical plate number (N) of

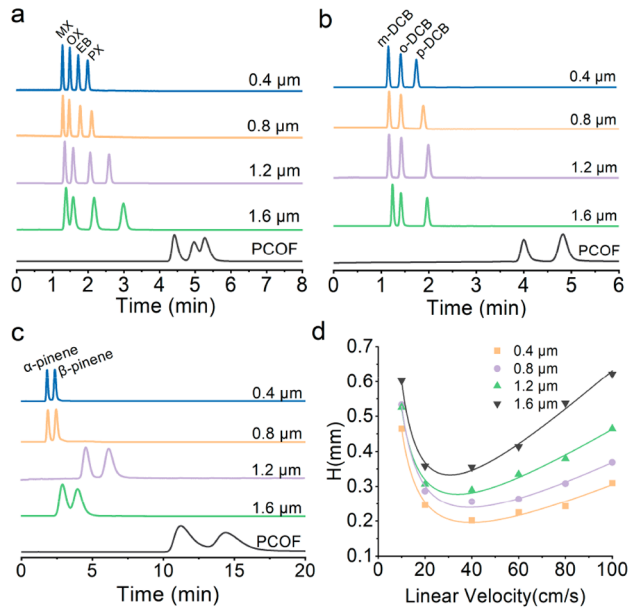

Figure 4. GC chromatograms of (a) xylene isomers (MX, OX, EB, and PX represented *m*-xylene, *o*-xylene, ethylbenzene, and *p*-xylene, respectively.), (b) DCB isomers, and (c) α-pinene and β-pinene on SCOF-303-capillaries with different particle sizes (10 m long × 0.53 mm i.d.). (d) Van Deemter plots of SCOF-303-capillaries with different particle sizes (Separation conditions were optimized to give the best separation of the isomer.).

SCOF-303-capillaries for *p*-xylene also decreased from 7879 to 4052 plates·m^{-1} with an increase in particle size (Table S3). The above trends of R and N were also observed in the separation of DCB and pinene (Tables S4−S5), indicating that larger particle size of SCOF-303 exhibited lower GC separation performance.

As SCOF-303 with different particle sizes owns the same composition and structure, the dominant separation force of SCOF-303-capillaries for the isomers including the hydrophobic interaction, $\pi-\pi$ interaction, and C−H···π interaction roughly remains the same.[13] Thus, the elution order of the isomers on different SCOF-303-capillaries was unchanged. COF-303 is well-known for its flexible structure, referring to the fact that the pore of COF-303 would dynamically change after the entrance of numerous guests. However, this flexibility attenuates with an increase in particle size, making the large particle size SCOF-303 rigid.[15,16] Thereby, the size-exclusion effect of large SCOF-303 would reduce, leading to a decrease in R. For example, kinetic diameters of xylene isomers are as follows: ethylbenzene (6.7 Å), *o*-xylene (7.4 Å), *m*-xylene (7.1 Å), and *p*-xylene (6.7 Å).[13] The dynamical structure change of SCOF-303 was mainly determined by the largest *o*-xylene. The less flexibility of large SCOF-303 exhibited the weaker size-exclusion effect for *o*-xylene, leading to the shorter retention. Thus, the R of *o*-xylene and *m*-xylene evidently decreased with an increase in particle size.

The Van Deemter equation can explain column efficiency from the kinetics factor.[25] Coefficients of eddy diffusion (A), longitudinal diffusion (B) and mass transfer resistance (C) of SCOF-303-capillaries with different particle sizes were calculated by measuring theoretical plate height (H) for n-butanol with different flow rates of N_2 (Figure 4d). The negligible A term resulted from the open-tubular columns of SCOF-303-capillaries.[26,27] According to Figure 4d, the curves tended to converge at a point with the low flow rate and became increasingly divergent at the high flow rate, indicating the dominance of the C term for H rather than the B term. In addition, the difference of fitted B values was not significant, while the C value decreased evidently from 0.30 to 0.62 ms with an increase in the particle size (Table S6), demonstrating that a decrease in the column efficiency of large particle size dominantly resulted from the strengthening of mass transfer resistance.

SCOF-303 with a particle size of 0.4 μm exhibited the best GC separation performance and, thus, was chosen to compare with commercial and other reported columns. All the isomers can be well separated on SCOF-303-capillary (0.4 μm) (Figure S10) but cannot be resolved on PCOF-303-capillary (Figure S11), indicating the generally superior separation of SCOF-303 to PCOF-303. Under the same column size, the broad-spectrum nonpolar commercial DB-5 capillary cannot give baseline separation of xylene and DCB isomers (Figure S12), and the recommended column HP-FFAP still cannot give baseline separation of xylene isomers (Figure S13). Moreover, comparison of SCOF-303 (0.4 μm) with many reported materials including HKUST-1, UiO-66, ZIF-8@PDMS, MAF-6, MCF-50, MOF-CJ3, PCL-Diol, GQDs, and KAPs-1[28−36] revealed superiority of SCOF-303 in R or separation time, fully demonstrating the high potential of SCOF-303-capillary in separation of isomers (Table S7).

Furthermore, repeatability and stability of SCOF-303-capillaries and PCOF-303-capillary were investigated. Run-to-run (n = 8) and day-to-day (n = 8) relative standard deviations

https://doi.org/10.1021/acs.analchem.3c01550
Anal. Chem. 2023, 95, 8145−8149

(RSDs) for the retention time of xylene isomers varies from 0.06%−0.39% (Table S8). Little reduction of N and capacity factor (k) (0.2%−2.0%) was observed after five temperature-programmed processes (Table S9). In contrast, PCOF-303-capillary gave larger RSDs and more reduction of N and k, indicating higher repeatability and stability of SCOF-303-capillaries.

In conclusion, we have first investigated the effect of particle size of SCOF on GC separation performance. The single-crystalline three-dimensional COF-303 bonded capillary was prepared via the in situ growth approach and proved to be superior to the PCOF-303-capillary for isomers of xylene, DCB, and pinene in R, N, and separation time. Comparison of SCOF-303-capillaries revealed the R and N for xylene, DCB, and pinene decreased with an increase in the particle size, dominantly resulting from that weaker size-exclusion effect and higher mass transfer resistance of larger SCOF-303. This work not only demonstrates the great potential of SCOFs as GC stationary phases but also provides new ideas and a method for further research to improve the performance of the COF based chromatographic column.

■ ASSOCIATED CONTENT

Supporting Information

The Supporting Information is available free of charge at https://pubs.acs.org/doi/10.1021/acs.analchem.3c01550.

Synthesis process for the powder and capillary of SCOF-303 and PCOF-303; Characterization of PCOF-303 capillary and SCOF-303-capillaries; Van't Hoff plots for SCOF-303-capillaries; GC chromatograms of SCOF-303-capillaries, PCOF-303-capillary and commercial capillaries; Comparison of the N and R, precision for the retention time, reduction of N and k, McReynolds constants and Van Deemter coefficients of SCOF-303-capillaries (PDF)

■ AUTHOR INFORMATION

Corresponding Author

Hai-Long Qian − *State Key Laboratory of Food Science and Technology, Jiangnan University, Wuxi 214122, China; Institute of Analytical Food Safety, School of Food Science and Technology, Jiangnan University, Wuxi 214122, China;* orcid.org/0000-0001-7554-4115; Email: hlqian@jiangnan.edu.cn

Authors

Zi-Han Wang − *Institute of Analytical Food Safety, School of Food Science and Technology, Jiangnan University, Wuxi 214122, China*

Cheng Yang − *State Key Laboratory of Food Science and Technology, Jiangnan University, Wuxi 214122, China; Institute of Analytical Food Safety, School of Food Science and Technology, Jiangnan University, Wuxi 214122, China*

Tianxi Liu − *Key Laboratory of Synthetic and Biological Colloids, Ministry of Education, School of Chemical and Material Engineering, Jiangnan University, Wuxi 214122, China*

Xiu-Ping Yan − *State Key Laboratory of Food Science and Technology, Jiangnan University, Wuxi 214122, China; Institute of Analytical Food Safety, School of Food Science and Technology and Key Laboratory of Synthetic and Biological Colloids, Ministry of Education, School of Chemical and Material Engineering, Jiangnan University, Wuxi 214122, China*

Complete contact information is available at: https://pubs.acs.org/10.1021/acs.analchem.3c01550

Notes

The authors declare no competing financial interest.

■ ACKNOWLEDGMENTS

This work was supported by the National Natural Science Foundation of China (nos. 22076066 and 22176073), the Program of "Collaborative Innovation Center of Food Safety and Quality Control in Jiangsu Province", and the "Fundamental Research Funds for the Central Universities".

■ REFERENCES

(1) Wu, Y.; Zhang, N.; Luo, K.; Liu, Y.; Bai, Z.; Tang, S. *TrAC-Trend. Anal. Chem.* **2022**, *153*, 116647.

(2) Mallik, A. K.; Qiu, H.; Takafuji, M.; Ihara, H. *TrAC-Trend. Anal. Chem.* **2018**, *108*, 381−404.

(3) Zhao, X.; Wang, Y. X.; Li, D. S.; Bu, X. H.; Feng, P. Y. *Adv. Mater.* **2018**, *30* (37), 1705189.

(4) Li, H.; Wang, X.; Shi, C.; Zhao, L.; Li, Z.; Qiu, H. *Chin. Chem. Lett.* **2023**, *34* (3), 107606.

(5) Cote, A. P.; Benin, A. I.; Ockwig, N. W.; O'Keeffe, M.; Matzger, A. J.; Yaghi, O. M. *Science* **2005**, *310* (5751), 1166−1170.

(6) Wu, M. X.; Yang, Y. W. *Chin. Chem. Lett.* **2017**, *28* (6), 1135−1143.

(7) Furukawa, H.; Yaghi, O. M. *J. Am. Chem. Soc.* **2009**, *131* (25), 8875−8883.

(8) Qian, H. L.; Yang, C. X.; Yan, X. P. *Nat. Commun.* **2016**, *7*, 12104.

(9) Waller, P. J.; Gandara, F.; Yaghi, O. M. *Acc. Chem. Res.* **2015**, *48* (12), 3053−3063.

(10) Liu, X.; Yang, C.; Qian, H. L.; Yan, X. P. *ACS Appl. Nano Mater.* **2021**, *4* (5), 5437−5443.

(11) Zheng, Q.; Liu, J.; Wu, Y.; Ji, Y.; Lin, Z. *Anal. Chem.* **2022**, *94* (51), 18067−18073.

(12) Ma, T. T.; Yang, C.; Qian, H. L.; Yan, X. P. *J. Chromatogr. A* **2022**, *1673*, 463085.

(13) Qian, H. L.; Wang, Z. H.; Yang, J.; Yan, X. P. *Chem. Commun.* **2022**, *58* (58), 8133−8136.

(14) Natraj, A.; Ji, W.; Xin, J.; Castano, I.; Burke, D. W.; Evans, A. M.; Strauss, M. J.; Ateia, M.; Hamachi, L. S.; Gianneschi, N. C.; Alothman, Z. A.; Sun, J.; Yusuf, K.; Dichtel, W. R. *J. Am. Chem. Soc.* **2022**, *144* (43), 19813−19824.

(15) Ma, T.; Kapustin, E. A.; Yin, S. X.; Liang, L.; Zhou, Z.; Niu, J.; Li, L. H.; Wang, Y.; Su, J.; Li, J.; Wang, X.; Wang, W. D.; Wang, W.; Sun, J.; Yaghi, O. M. *Science* **2018**, *361* (6397), 48−52.

(16) Ma, T.; Wei, L.; Liang, L.; Yin, S.; Xu, L.; Niu, J.; Xue, H.; Wang, X.; Sun, J.; Zhang, Y. B.; Wang, W. *Nat. Commun.* **2020**, *11* (1), 6128.

(17) Zhang, Y. B.; Su, J.; Furukawa, H.; Yun, Y.; Gandara, F.; Duong, A.; Zou, X.; Yaghi, O. M. *J. Am. Chem. Soc.* **2013**, *135* (44), 16336−16339.

(18) Evans, A. M.; Parent, L. R.; Flanders, N. C.; Bisbey, R. P.; Vitaku, E.; Kirschner, M. S.; Schaller, R. D.; Chen, L. X.; Gianneschi, N. C.; Dichtel, W. R. *Science* **2018**, *361* (6397), 52−57.

(19) Liu, T.; Zhao, Y.; Song, M.; Pang, X.; Shi, X.; Jia, J.; Chi, L.; Lu, G. *J. Am. Chem. Soc.* **2023**, *145* (4), 2544−2552.

(20) Chen, Y. C.; Shi, Z. L.; Wei, L.; Zhou, B. B.; Tan, J.; Zhou, H. L.; Zhang, Y. B. *J. Am. Chem. Soc.* **2019**, *141* (7), 3298−3303.

(21) Sun, T.; Wei, L.; Chen, Y. C.; Ma, Y. H.; Zhang, Y. B. *J. Am. Chem. Soc.* **2019**, *141* (28), 10962−10966.

(22) Zheng, Q.; Huang, J.; He, Y.; Huang, H.; Ji, Y.; Zhang, Y.; Lin, Z. *Acs Appl. Mater. Interfaces* **2022**, *14* (7), 9754−9762.

(23) McReynolds, M. O. *J. Chromatogr. Sci.* **1970**, *8* (12), 685−691.

(24) Kollie, T. O.; Poole, C. F.; Abraham, M. H.; Whiting, G. S. *Anal. Chim. Acta* **1992**, *259* (1), 1−13.
(25) VanDeemter, J. J. *Chem. Eng. Sci.* **1995**, *50* (24), 3867−3867.
(26) Blumberg, L. M. *J. Chromatogr. A* **2017**, *1524*, 303−306.
(27) Berezkin, V. G.; Malyukova, I. V.; Avoce, D. S. *J. Chromatogr. A* **2000**, *872* (1−2), 111−118.
(28) Munch, A. S.; Mertens, F. *J. Mater. Chem.* **2012**, *22* (20), 10228−10234.
(29) Chang, N.; Yan, X. P. *J. Chromatogr. A* **2012**, *1257*, 116−124.
(30) Srivastava, M.; Roy, P. K.; Ramanan, A. *RSC Adv.* **2016**, *6* (16), 13426−13432.
(31) He, C. T.; Jiang, L.; Ye, Z. M.; Krishna, R.; Zhong, Z. S.; Liao, P. Q.; Xu, J. Q.; Ouyang, G. F.; Zhang, J. P.; Chen, X. M. *J. Am. Chem. Soc.* **2015**, *137* (22), 7217−7223.
(32) Lin, J. M.; He, C. T.; Liao, P. Q.; Lin, R. B.; Zhang, J. P. *Sci. Rep.* **2015**, *5*, 11537.
(33) Fang, Z. L.; Zheng, S. R.; Tan, J. B.; Cai, S. L.; Fan, J.; Yan, X.; Zhang, W. G. *J. Chromatogr. A* **2013**, *1285*, 132−138.
(34) Peng, J.; Zhang, Y.; Yang, X.; Qi, M. *J. Chromatogr. A* **2016**, *1466*, 148−154.
(35) Lu, C.; Liu, S.; Xu, J.; Ding, Y.; Ouyang, G. *Anal. Chim. Acta* **2016**, *902*, 205−211.
(36) Zhang, X.; Ji, H.; Zhang, X.; Wang, Z.; Xiao, D. *Anal. Methods* **2015**, *7* (7), 3229−3237.

https://doi.org/10.1021/acs.analchem.3c01550
Anal. Chem. 2023, 95, 8145−8149